



CCD series no-19: The lowest energy prospects for SWRO through single-element modules under plug-flow and closed-circuit desalination conditions

Avi Efraty

Desalitech Ltd, P.O. Box 132, Har-Adar 90836, Israel, email: avi@desalitech.com

Received 26 March 2015; Accepted 22 November 2015

ABSTRACT

The future targets of the SWRO desalination industry to reduce significantly energy consumption are realized already today by the newly emerging closed-circuit desalination (CCD) technology with demonstrated energy consumption of 2.12 kWh/m³ for Mediterranean water (4.0%) and 1.72 kWh/m³ for ocean (3.5%) water without the need for energy recovery with energy saving greater than 35%. The fundamental differences between CCD and the conventional plug flow desalination (PFD) techniques are evaluated in the present study by rigorous theoretical model simulations of CCD compared with multi-stage PFD of the same single-element modules under the same conditions in the flux range of 13.0–0.1 lmh. The results of this study reveal that CCD under fixed flow and variable pressure conditions behaves as near-perfect multi-stage PFD with energy dependence on recovery also manifesting increased frequency of CCD cycles and residence time. The origin of energy savings by CCD and multi-stage PFD compared with conventional single-pass through multi-element module is revealed and explained. While multi-stage SWRO designs are economically prohibited by high fabrication costs, CCD designs are simple and inexpensive and should play a major role in future design of SWRO desalination plants of low energy consumption and high energy conversion efficiency without the need of ERD.

Keywords: Seawater desalination energy; Low-energy SWRO desalination; Closed-circuit desalination (CCD); SWRO-CCD of low energy; Entropy efficiency of SWRO desalination; Entropy efficiency of SWRO-CCD

1. Introduction

Most of the Earth's surface (~70%) is covered by seawater which represents ~99% of water on our planet with only a small fraction (<1.0%) found as ground and surface water in the forms of freshwater (FW) and/or brackish water (BW). Depletion/deterioration of FW sources on Earth due to increased demand/consumption by expanding global population, adverse regional climate changes, and growing

pollution, created an increased reliance on RO desalination of seawater (SWRO) and BW (BWRO) for the creation of FW supplements, evident already worldwide. SWRO desalination [1] became the method of choice for the creation of FW supplement in many coastal regions worldwide where scarcity of FW supplies is experienced and the same also apply to BWRO desalination since such processes are greatly preferred thermodynamically [2] over alternative desalination techniques. The expanding global desalination

industry with rate growth of 10–12% per annum relies primarily on conventional plug flow desalination (PFD) techniques which remain essentially unchanged since inception by Loeb and Sourirajan [3] and practised today at near-state-of-the-art with very little room for further improvements as results of the utilization of advance membranes and efficient pumps and energy recovery means (ERD) from the pressurized brine effluent. Conventional SWRO of 45–50% is normally practised by a single-pass process with modules of eight elements, whereas such BWRO processes proceed with ~80% recovery using two-stage designs and up to 90% recovery using three-stage designs with modules of six elements each with energy consumption determined by the fixed pressure feed at inlet (10–20% above that of the osmotic pressure of the brine effluent) and by the efficiency of pumps and ERD. Future goals/targets of the desalination industry [4] require RO processes of significantly lower energy and increased recovery and this implies the need to development new techniques to meet stated future objectives.

Closed-circuit desalination (CCD) is a noteworthy recently emerging new RO technology of different operational principles compared with PFD which was demonstrated already for SW [5–14] and BW [15–24] applications and meets all future goals/targets of the desalination industry [4]. CCD is a batch desalination process carried out under fixed flow and variable pressure conditions where the entire concentrate is recycled and mixed with fresh pressurized feed at module(s) inlet(s). Energy consumption by this technology is progressively supplied as function of increased batch desalination requirements and recovery is a function of concentrate recycling irrespective of the number of elements per module. Since pressurized brine is not emitted during the CCD batch desalination process, there is no need for ERD and such processes proceed with near-absolute energy conversion efficiency. Commercial application of CCD was made possible by the development of consecutive sequential batch desalination techniques and in the light of their present and future prospects to the desalination industry, the understanding of the theoretical and practical aspects of CCD received considerable attention in recent years [5–24].

A recent theoretical study by Lin and Elimelech [25] analyzed the minimum specific energy (SE) of desalination dependence on the number of steps of conventional multi-stage PFD and CCD processes in order to elucidate the fundamental differences between these methods and concluded "... that although it is theoretical impossible to reach the thermodynamic minimum energy of separation with

closed-circuit RO, this configuration is robust and much more practical to implement than the multi-stage direct pass RO". While the study of Lin and Elimelech focuses primarily on the minimum energy requirements of multi-step PFD and CCD processes under infinitesimal flux conditions, it was thought to be of interest to compare such SWRO processes under real operational conditions in the flux range of 13.0–0.1 l/mh and such a comprehensive theoretical study is described in the present study at the level of multi-step processes with identical single-element modules.

2. Low-energy multi-step SWRO-PFD and CCD desalination processes

Conventional SWRO-PFD is carried out with module of eight elements in line (ME8) according to the schematic design in Fig. 1(A) and the ideal multi-stage process with single-element modules (ME) of the design depicted in Fig. 1(B) which with its inter-stage pressure boosting means is expected to allow the lowest energy pathway for seawater desalination. In contrast with the multi-stage PFD, the CCD technology under fixed flow and variable pressure conditions behaves as a perfect-staged flow and pressure-boosted technology with recovery determined only by the number of concentrate recycling steps irrespective of the number of elements per module and/or the selected flux of operation, including at the basic level of the single-element design displayed in Fig. 1(C). Accordingly, the theoretical model study under review relates to the recovery-dependend performance of the multi-stage PDF design in Fig. 1(B) as compared with that of the CCD design in Fig. 1(C) with the same single-element modules (ME) under identical flux and module recovery (MR) conditions.

While the schematic design in Fig. 1(B), which illustrates the multi-stage equivalent of the conventional SWRO-PFD design in Fig. 1(A), looks relatively simple, the attainment of a near-perfect flow design of the same inlet and outlet flow rates per single-element modules in the design is a rather complex issue and requires an enormous number of modules per stage. For instance, the attainment of near-identical flow conditions in all the equivalent single-element modules depicted in Fig. 1(B) with an assumed 10% module recovery (MR) and 50% recovery of the entire array would require 1,000 ME (S1); 900 ME (S2); 810 ME (S3); 729 ME (S4); 656 ME (S5); 590 ME (S6); 531 ME (S7); and 478 ME (S8) with a total of 5,894 ME for the entire design with stage (S) number indicated in parenthesis. In contrast, attainment of fixed flow rates per desired MR during CCD cycles is achieved by control means independent of the number of elements

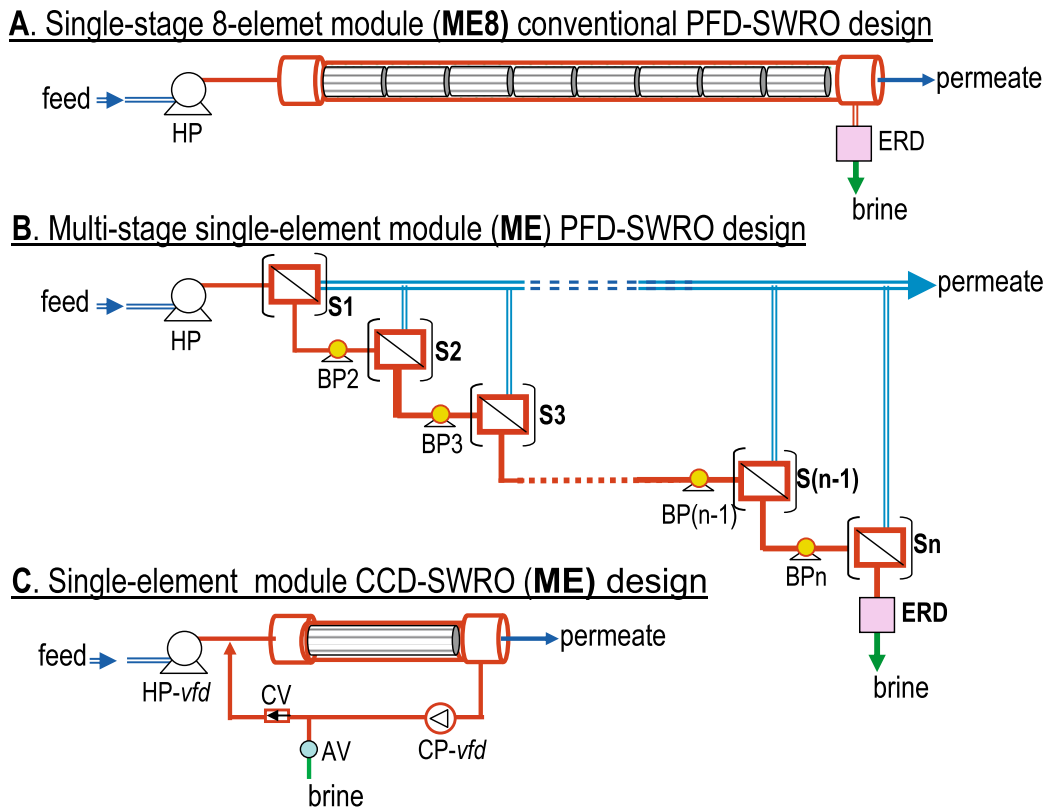


Fig. 1. Schematic illustrations of a single-stage eight-element module (ME8) conventional PFD-SWRO design (A); a multi-stage (n) single-element module (ME) PFD-SWRO design (B), and a single-element module (ME) CCD-SWRO design (C). Abbreviations: S, stage; n , stage number; HP, high-pressure pump; CP, circulation pump; BP, booster pump; ERD, energy recovery device; *vfd*, variable frequency drive; CV, check valve; and AV, actuated valve. Red color describes pressurized sections and blue or green colors, non-pressurized sections with green reserved for brine.

per module and/or the ultimate consecutive batch recovery and these features allow to compare the ME module performance in Fig. 1(C) design to that in Fig. 1(B) design under exactly the same conditions.

3. Model simulations for ME in CCD and multi-stage PFD processes

The theoretical model simulation database for the CCD process according to Fig. 1(C) design is displayed in Table 1A with each column in the table labeled at bottom by a number. Selected data at the top of the table (yellow background) outline the module configuration (single-element module), membrane type (SWC6-MAX) and its test conditions, feed source concentration (3.5% typical of ocean water), flux (13 lmh), MR (10%), temperature (25°C), efficiency of pumps (85% HP and 75% CP), and the van't-Hoff constant for conversion of percent seawater concentrations to osmotic pressures (7.43 bar/%). The selected operational parameters lead to the listed theoretically

calculated terms of flow rates (Q), module pressure difference (Δp), average module recovery per element ($av\text{-MR}/\text{Element}$), average concentration polarization factor ($av\text{-}pf$), cycle time duration (min/cycle), and average permeate production per cycle (m^3/cycle). CCD module inlet concentrations per cycle (3A) are derived from the module outlet concentrations (4A) by means of mass balance which takes into account the dilution effect at module inlet. The applied pressure (p_a) per cycle (6A) is derived by (1), where μ stands for flux, A for permeability coefficient, T_{CF} for temperature correction factor, $\Delta\pi_{av}$ for average osmotic pressure of concentrate, Δp for module pressure difference, p_p for permeate pressure release, and π_p for osmotic pressure of permeate. The average applied pressure (7A) is derived from the applied pressure per cycle (6A). The power expressions of pumps (8A–10A) are the products of pressure and flow, and the average specific energy contribution of the major power source in the system ($av\text{-HP}$) in 11A is a sole function of the average pressure (7A). The batch sequence cumulative

Table 1

Theoretical model simulation data for ME (E = SWC6-MAX) in CCD (A) and in multi-stage PFD (B) for seawater (3.5%–26 bar π) desalination with 13 lmh flux and 10% MR at cited temperature and efficiency of pumps

TEST - SWC6 MAX		UNIT DESIGN		CCD Parameters		Temperature	
40.8	m ² /Element	1	Modules	3.50	% Initial feed	Temp	25 °C
50	m ³ /day	1	Elements/Module	13.0	lmh Flux	TCF	1.000 factor
32,000	ppm NaCl	120	cm long PV		0.53 m ³ /h Permeate (=Q _{HP})		
54	bar Applied Pressure	20	cm diameter PV	10.0	% Module Recovery		
10	% Recovery	15	liter element volume		4.77 m ³ /h Q _{cp}		
25	Centigrade	5	% lines volume		5.30 m ³ /h Module Inlet flow		
99.80	% Salt Rejection		23.8 liter per module		0.106 bar Δp		
30.229	bar NDP				0.30 min/cycle		
51.062	l/m ² /h Flux	π (bar)-C(%)			0.0026 m ³ /cycle of permeate		
1.6892	l/m ² /h/bar -A	35,000	ppm Ocean water Feed		0.100 av-MR/Element		0.85 HP eff.
0.0802	l/m ² /h - B	26.00	bar Osmotic Pressure		1.035 av-pf		0.75 CP eff.
			7.43 π (bar)/C(%) - van't Hoff factor		10.00 Flow ratio(concentrate/permeate)		

A: CCD simulation results

Steps & Concentrations			CCD Sequence Cycles							CCD Sequence Combined				Permeate		Entorpy	
Mode	cycle	Inlet %	Outlet %	Time min	Applied (p _a)		Power (kW) per cycle			av-HP kWh/m ³	PERM Σ m ³	avergae		REC %	Cycle ppm	average ppm	Efficiency %
					bar	av-bar	HP	CP	HP+CP			Σ kWh	kWh/m ³				
CCD	0	3.50	3.50	0.0	34.7	34.7	0.601	0.019	0.620	1.133	0.000	0	1.155	0	223	223	62.51
CCD	1	3.50	3.89	0.3	36.2	36.2	0.627	0.019	0.646	1.18	0.003	0.646	1.217	10.0	236	236	59.34
CCD	2	3.85	4.28	0.6	39.0	37.6	0.676	0.019	0.695	1.23	0.005	0.670	1.264	18.2	259	248	57.16
CCD	3	4.20	4.67	0.9	41.8	39.0	0.725	0.019	0.744	1.27	0.008	0.695	1.310	25.0	283	259	55.13
CCD	4	4.55	5.06	1.2	44.7	40.4	0.774	0.019	0.793	1.32	0.011	0.719	1.356	30.8	307	271	53.25
CCD	5	4.90	5.44	1.5	47.5	41.8	0.824	0.019	0.843	1.37	0.013	0.744	1.403	35.7	330	283	51.49
CCD	6	5.25	5.83	1.8	50.4	43.3	0.873	0.019	0.892	1.41	0.016	0.769	1.449	40.0	354	295	49.84
CCD	7	5.60	6.22	2.1	53.2	44.7	0.922	0.019	0.941	1.46	0.019	0.793	1.496	43.8	377	307	48.29
CCD	8	5.95	6.61	2.4	56.0	46.1	0.971	0.019	0.990	1.51	0.021	0.818	1.542	47.1	401	318	46.84
CCD	9	6.30	7.00	2.7	58.9	47.5	1.021	0.019	1.039	1.55	0.024	0.843	1.588	50.0	425	330	45.47
CCD	10	6.65	7.39	3.0	61.7	48.9	1.070	0.019	1.089	1.60	0.026	0.867	1.635	52.6	448	342	44.18
CCD	11	7.00	7.78	3.3	64.6	50.4	1.119	0.019	1.138	1.65	0.029	0.892	1.681	55.0	472	354	42.96
CCD	12	7.35	8.17	3.6	67.4	51.8	1.168	0.019	1.187	1.69	0.032	0.916	1.728	57.1	495	366	41.80
CCD	13	7.70	8.56	3.9	70.2	53.2	1.218	0.019	1.236	1.74	0.034	0.941	1.774	59.1	519	377	40.71
CCD	14	8.05	8.94	4.2	73.1	54.6	1.267	0.019	1.286	1.79	0.037	0.966	1.821	60.9	543	389	39.67
CCD	15	8.40	9.33	4.5	75.9	56.0	1.316	0.019	1.335	1.83	0.040	0.990	1.867	62.5	566	401	38.68
CCD	16	8.75	9.72	4.8	78.8	57.5	1.365	0.019	1.384	1.88	0.042	1.015	1.913	64.0	590	413	37.75
CCD	17	9.10	10.11	5.1	81.6	58.9	1.415	0.019	1.433	1.92	0.045	1.039	1.960	65.4	613	425	36.85
CCD	18	9.45	10.50	5.4	84.5	60.3	1.464	0.019	1.483	1.97	0.048	1.064	2.006	66.7	637	436	36.00
CCD	19	9.80	10.89	5.7	87.3	61.7	1.513	0.019	1.532	2.02	0.050	1.089	2.053	67.9	661	448	35.18
CCD	20	10.15	11.28	6.0	90.1	63.1	1.562	0.019	1.581	2.06	0.053	1.113	2.099	69.0	684	460	34.41
CCD	21	10.50	11.67	6.3	93.0	64.6	1.612	0.019	1.630	2.11	0.056	1.138	2.145	70.0	708	472	33.66
CCD	22	10.85	12.06	6.6	95.8	66.0	1.661	0.019	1.680	2.16	0.058	1.163	2.192	71.0	731	484	32.95
CCD	23	11.20	12.44	6.9	98.7	67.4	1.710	0.019	1.729	2.20	0.061	1.187	2.238	71.9	755	495	32.27
1A	2A	3A	4A	5A	6A	7A	8A	9A	10A	11A	12A	13A	14A	15A	16A	17A	18A

B: Multi-stage PFD simulation results

Step		Flow rates			Concentrations		Pressure		Energy, recovery and TDS of permeates					Entropy
		inlet	PERM	Outlet	inlet	outlet	p_a	Δp_a	SE	av-SE	REC	Stage	average	Efficiency
Mode	Stage	m ³ /h	m ³ /h	m ³ /h	%	%	bar	bar	kWh/m ³	kWh/m ³	%	ppm	ppm	%
PFD	0	5.30	0.53		3.50	3.50	34.7		1.13	1.133	0.00			63.76
PFD	1	5.30	0.53	4.77	3.50	3.89	36.2		1.18	1.182	10.00	236	236	61.12
PFD	2	5.30	0.53	4.77	3.89	4.32	39.3	3.2	1.28	1.233	19.00	250	243	58.56
PFD	3	5.30	0.53	4.77	4.32	4.80	42.8	3.5	1.40	1.289	27.10	265	250	56.05
PFD	4	5.30	0.53	4.77	4.80	5.33	46.7	3.9	1.53	1.348	34.39	282	258	53.57
PFD	5	5.30	0.53	4.77	5.33	5.93	51.0	4.3	1.67	1.412	40.95	301	267	51.14
PFD	6	5.30	0.53	4.77	5.93	6.59	55.9	4.8	1.83	1.481	46.86	322	276	48.76
PFD	7	5.30	0.53	4.77	6.59	7.32	61.2	5.3	2.00	1.555	52.17	345	286	46.44
PFD	8	5.30	0.53	4.77	7.32	8.13	67.1	5.9	2.19	1.635	56.95	371	297	44.17
PFD	9	5.30	0.53	4.77	8.13	9.03	73.7	6.6	2.41	1.721	61.26	400	308	41.96
PFD	10	5.30	0.53	4.77	9.03	10.04	81.1	7.3	2.65	1.814	65.13	432	320	39.81
PFD	11	5.30	0.53	4.77	10.04	11.15	89.2	8.1	2.92	1.914	68.62	468	334	37.73
PFD	12	5.30	0.53	4.77	11.15	12.39	98.3	9.1	3.21	2.022	71.76	507	348	35.71
1B	2B	3B	4B	5B	6B	7B	8B	9B	10B	11B	12B	13B	14B	15B

terms of permeate volume (Σm^3) production (12A) and total (HP + CP) energy (ΣkWh) consumption (13A) which take into account the sequence time progression (5A), yield the av-SE per recovery level during the batch desalination progression (14A), which is found only slightly higher than the respective av-SE contributions of HP (11A). The CCD batch recovery (R_{BR}) terms in the table (15A) are derived by (2), where ΣV_p stand for Σm^3 of permeates (12A) and V_i for the cited intrinsic volume of the closed circuit (23.8 L) at the top of the table. The permeate TDS terms per cycle (16A) and average (17A) in the table are derived by (3), where C_p stands for permeate concentration, B for salt diffusion coefficient, and C_f for module feed concentration. The entropy efficiency (EE) terms (18A) are derived by (4), where $W_{least-min}$ stands for the least-minimum SE of separation under reversible infinitesimal flux conditions and W_{sep} for the actual SE of separation. The least-minimum SE is the minimum energy required to overcome the osmotic pressure of source under reversible infinitesimal flux conditions, or 26 bar·m³ (0.722 kWh/m³) for ocean seawater (3.5% and $\pi_f = 26$ bar).

$$p_a = \mu/A/T_{CF} + \Delta\pi_{av} + \Delta p/2 + p_p - \pi_p \quad (1)$$

$$R_{BR} = 100 \times \sum V_p / (\sum V_p + V_i) \quad (2)$$

$$C_p = B \times C_f \times pf \times T_{CF}/\mu \quad (3)$$

$$EE = 100 \times [W_{least-min}/W_{sep}] \quad (4)$$

The data presented in Table 1B pertains to a perfect multi-stage PFD process of single-element modules ME (E = SWC6-MAX) and flow rates per module (3B-5B) the same as for the CCD process. Module inlet (6B) and outlet (7B) concentrations per stage are defined by MR (10%) which is the same as for CCD. The applied pressure (p_a) per stage in Table 1B (8B) is derived by (1) with the same selected flux (13 lmh) as for the CCD process and the boosted pressure per stage (9B) is pressure difference (Δp_a) of successive stages. All the modules of the staged PFD design operate with identical flow rates, irrespective of stage, and the SE of separation per stage is defined only from the product of applied pressure and permeate volume ($p_a \times V$, bar \times m³), and the data in the table (10B) in kWh/m³ are derived from the expression $p_a/36/\text{eff}_{HP}$. Recovery in the multi-stage process under review proceeds along the line of staged ME modules of the same MR and the SE of the entire process is manifested by the average of all stages (11B). The cumulative recovery (12B) during the process is well defined from the feed and brine concentrations in the process, and the percent EE terms of the staged process (15B) are derived by (4) as already explained for CCD. The permeate TDS terms per cycle (13B) in the table are derived by (3) and the average values (14B)

take into account the relative permeate production per stage.

The simulated data in Table 1A for ME CCD and in Table 1B for ME multi-stage PFD reveal that both processes are compared under identical flow rates and flux conditions. The same simulation database may apply to compare said processes under different flux conditions by entering the desired flux at the stop of Table 1A and such simulations were repeated also for low flux (e.g. 0.3 and 0.1 lmh) in order to ascertain the comparative performance under near-infinitesimal flux conditions.

4. Model simulation results of compared CCD and multi-stage PFD processes

The results of single-element modules (ME) CCD and multi-stage PFD desalination simulations for seawater (3.5–26 bar π) at 13 lmh [Table 1(AB)] as well as at 0.3 lmh on the recovery scale under identical conditions ($\text{eff}_{\text{HP}} = \text{eff}_{\text{BP}} = 85\%$, $\text{eff}_{\text{CP}} = 75\%$, and $\text{eff}_{\text{ERD}} = 100\%$, as appropriate) are displayed in Fig. 2(A) and (B) for module concentrations, in Fig. 3(A) and (B) for pressures; in Fig. 4(A) and (B) for

specific energies; in Fig. 5(A) and (B) for percent entropy efficiencies; in Fig. 6(A) and (B) for TDS of permeates; in Fig. 7(A) and (B) for number of steps (PFD stages or CCD cycles); and in Fig. 8(AB) for residence time at 13 lmh (A) and 0.3 lmh (B).

The results in Fig. 2(A) and (B) reveal the same ME module concentrations irrespective of flux and the same applied pressure for PFD and CCD at a defined flux in Fig. 3(A) and (B) with decreased pressure concomitant with declined flux and the ultimate merge of the pressure curves at near-infinitesimal flux of 0.3 lmh as expected by theory for a thermodynamically reversible desalination process under infinitesimal flux conditions. The average specific energy of the compared designs in Fig. 4(A) and (B) reveal a slightly lower energy for the multi-stage PFD design (Fig. 1(B)) irrespective of flux due to the small energy consumption of the circulation pump (CP) in the CCD design (Fig. 1(C)), with declined flux affecting lower energies. The energy spread between the similar average specific energy curves of PFD and CCD and the theory minimum specific energy on the basis of the average osmotic pressure of concentrates declines with flux, and Fig. 4(B) manifests energy losses arising from

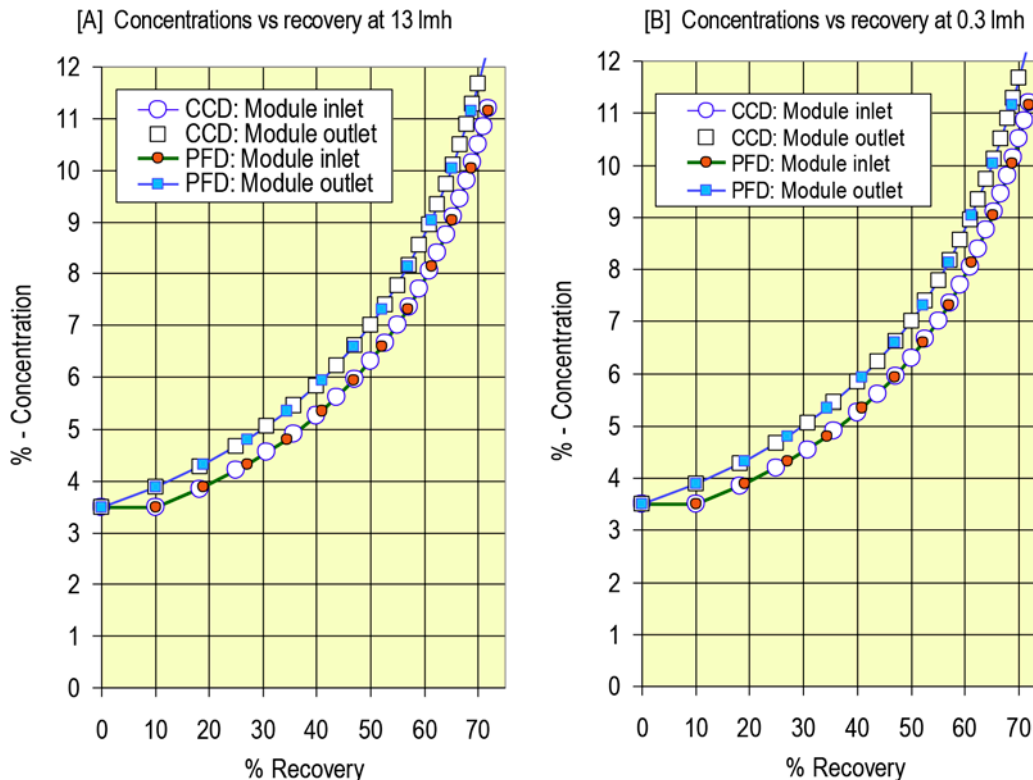


Fig. 2. Module concentrations vs. recovery for 13 lmh (A) and 0.3 lmh (B) according to the simulation database in Table 1(AB).

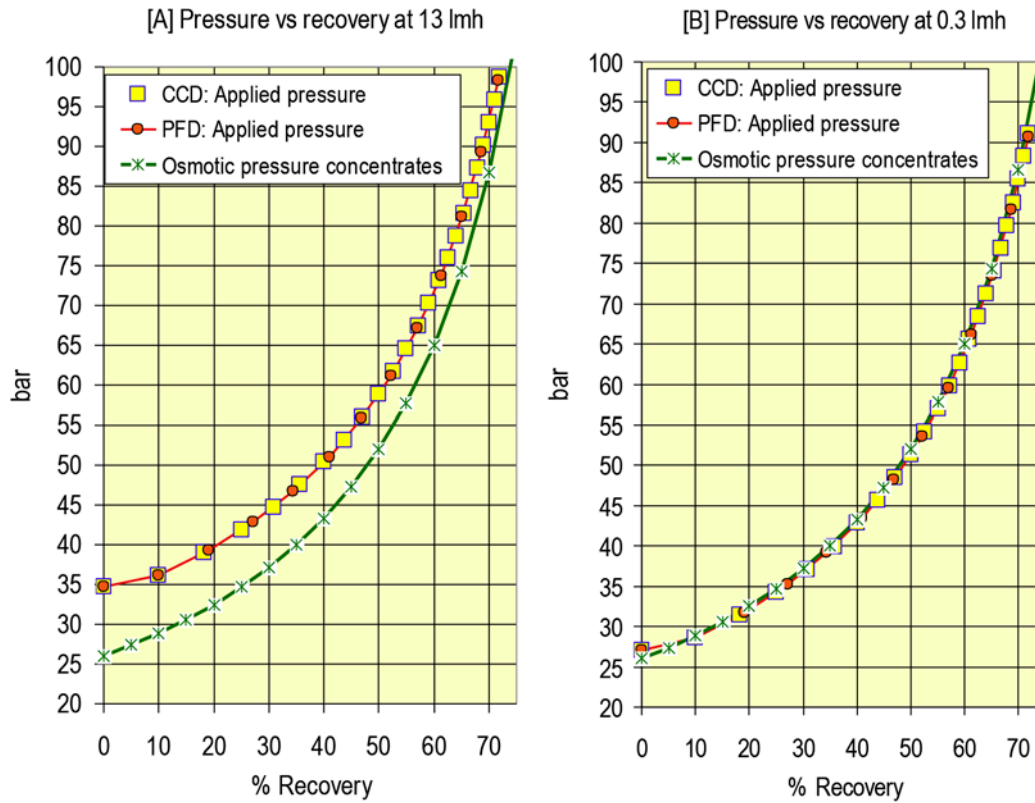


Fig. 3. Pressures vs. recovery for 13 lmh (A) and 0.3 lmh (B) according to the simulation database in Table 1(AB).

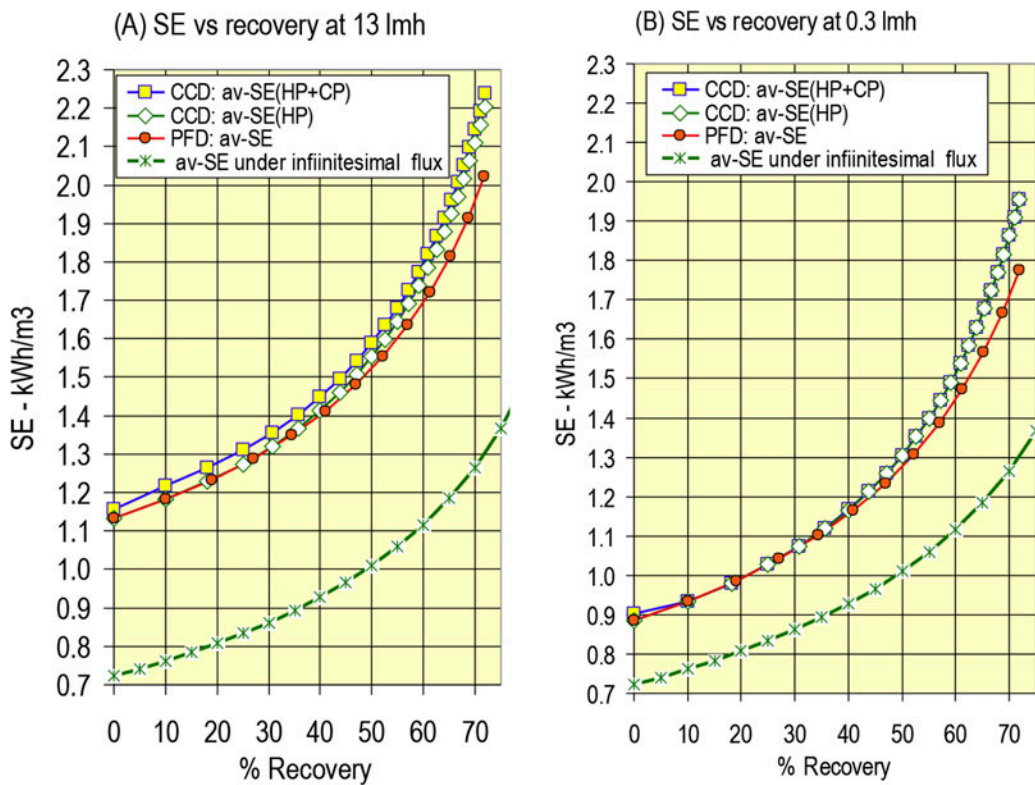


Fig. 4. Specific energies vs. recovery for 13 lmh (A) and 0.3 lmh (B) according to the simulation database in Table 1(AB).

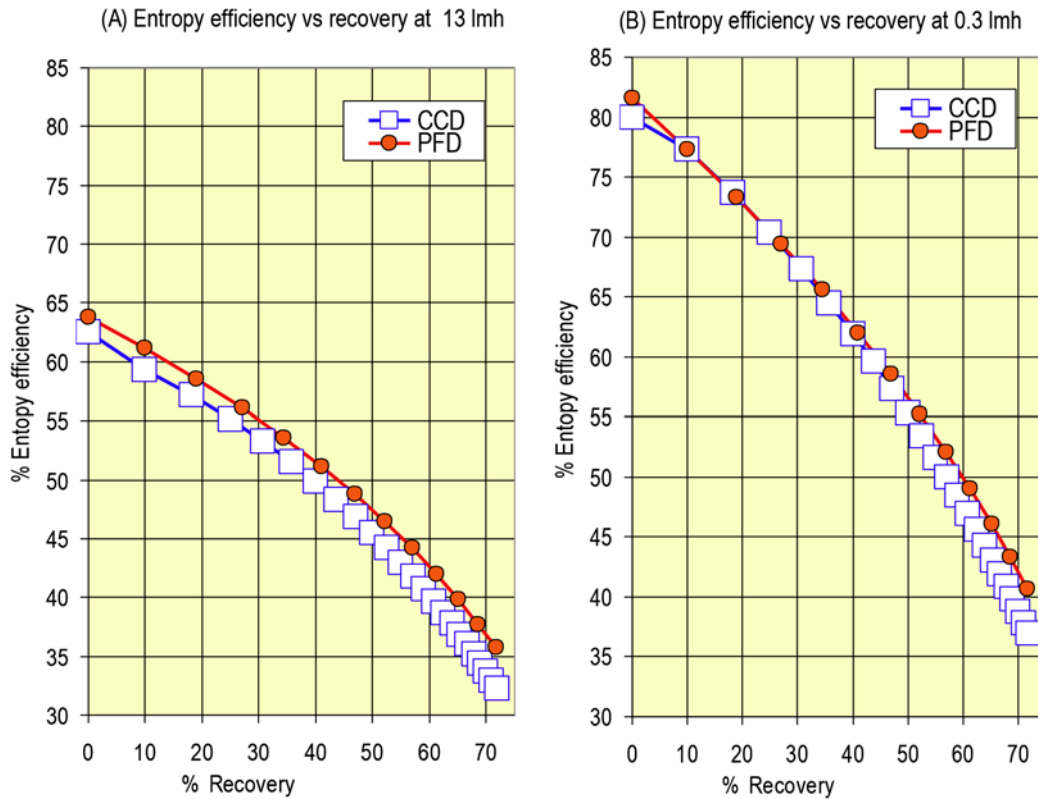


Fig. 5. EE vs. recovery for 13 lmh (A) and 0.3 lmh (B) according to the simulation database in Table 1(AB).

the efficiency of pumps. EE comparison in Fig. 5(A) and (B) shows a slight advantage in favor of the multi-step PFD over CCD as well as dependence on flux with maximum such efficiency experienced under near-infinitesimal flux conditions displayed in Fig. 5(B). Average TDS of permeates displayed in Fig. 6(A) and (B) reveals inferior permeates for CCD with dramatically high TDS values under near-infinitesimal flux conditions as expected by theory according to expression (3). The number of steps (stages of multi-stage PFD and cycles in CCD) required to reach a certain recovery is greater for CCD and associated with a longer residence time according to Figs. 7(A) and (B) and 8(A) and (B), respectively. Increased number of steps associated with and longer residence time under the same flux conditions experience in CCD compared with the multi-stage PFD clearly explains the inferior permeates quality produced by the former, although such permeates could be improved by increased flux which in case of CCD achieved by a simple set-point control change independent of MR, batch recovery, and cross-flow.

The pressure and energy aspects of the comparative study between multi-step PFD and CCD are of particular interest in the context of seawater desalina-

tion by RO, a process of high pressure which consumes considerable amounts of energy and the saving of energy in such a process is a major present and future target of the desalination industry. Energy consumption in the compared processes under review depends on flux and efficiency of pumps and the results obtained for absolute efficiency of pumps (100%) and for 13.0, 6.5, and 0.1 lmh flux by the appropriate modification of the database in Table (AB) are displayed for pressures in Fig. 9(A)–(C) and for specific energies in Fig. 10(A)–(C). Noteworthy in Fig. 9(A)–(C) are the demising gaps between osmotic pressures of concentrates and average applied pressures with declined flux and their ultimate merge at near-infinitesimal flux (0.1 lmh) as well as the similar behaviors with regard to specific energies displayed in Fig. 10(A)–(C).

5. Discussion

The comparative theoretical model results on the basis of the database in Table 1(AB) when applied to seawater RO desalination reveal similar applied pressures (Fig. 3(A) and (B)) for the flow-staged and pressure-boosted CCD design (Fig. 1(C)) of a

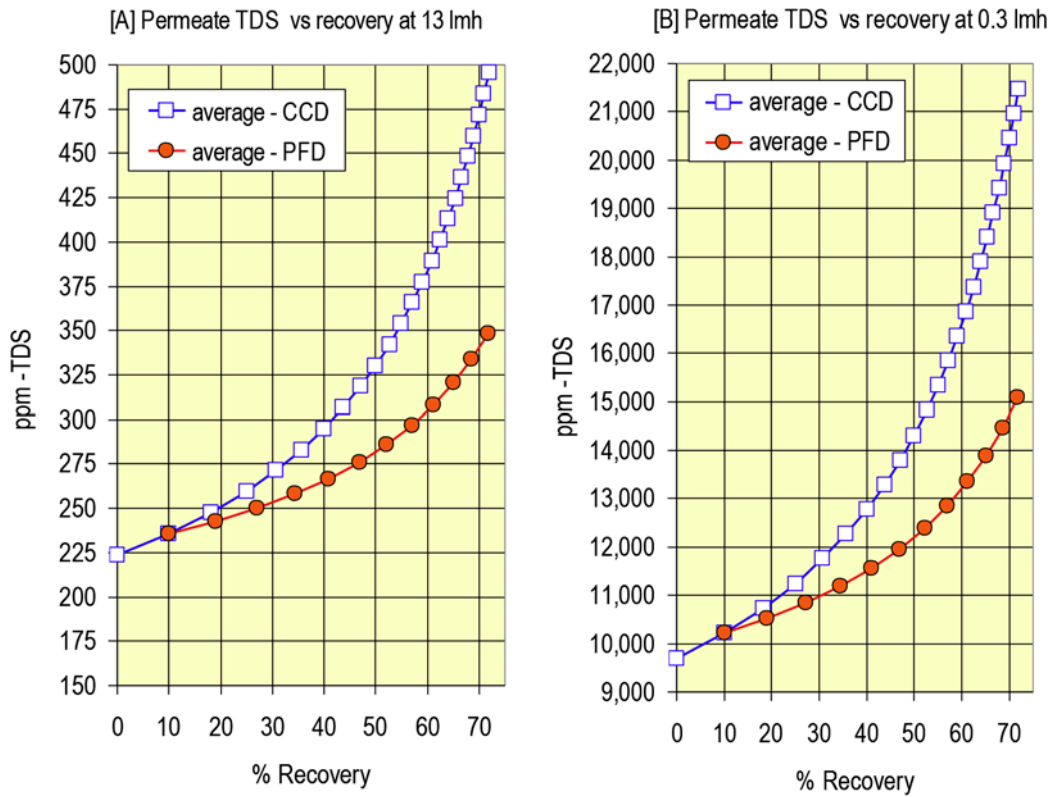


Fig. 6. TDS of permeates vs. recovery for 13 lmh (A) and 0.3 lmh (B) according to the simulation database in Table 1(AB).

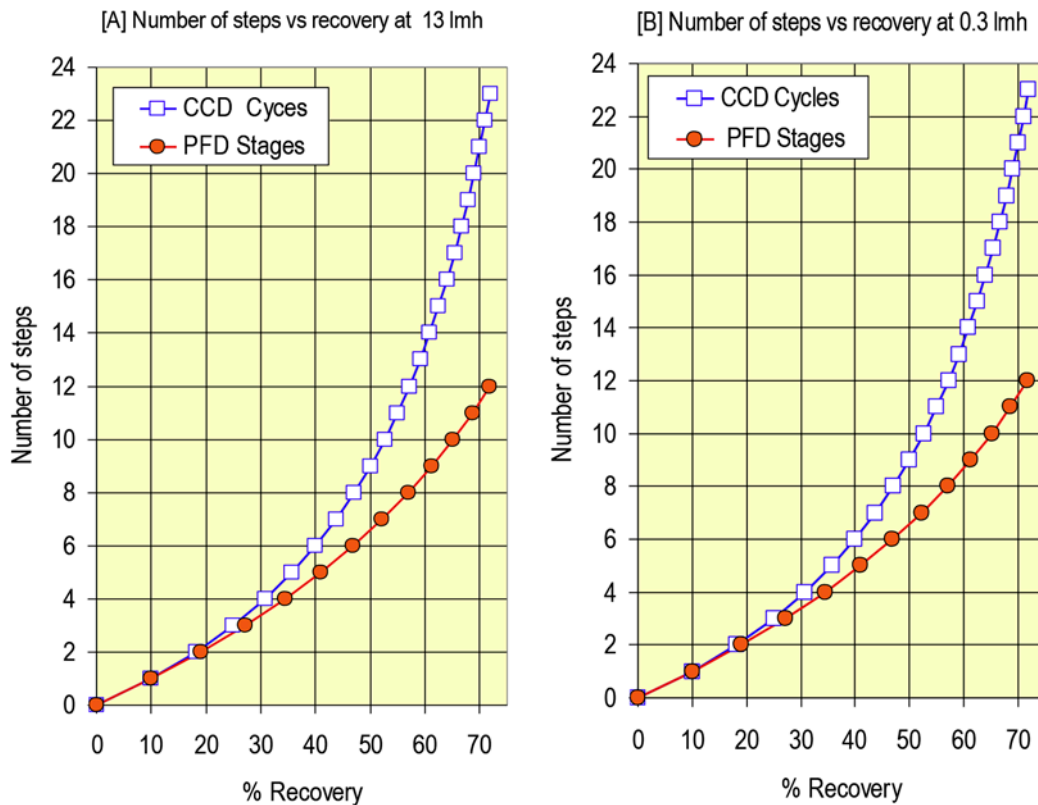


Fig. 7. Number of steps vs. recovery for 13 lmh (A) and 0.3 lmh (B) according to the simulation database in Table 1(AB).

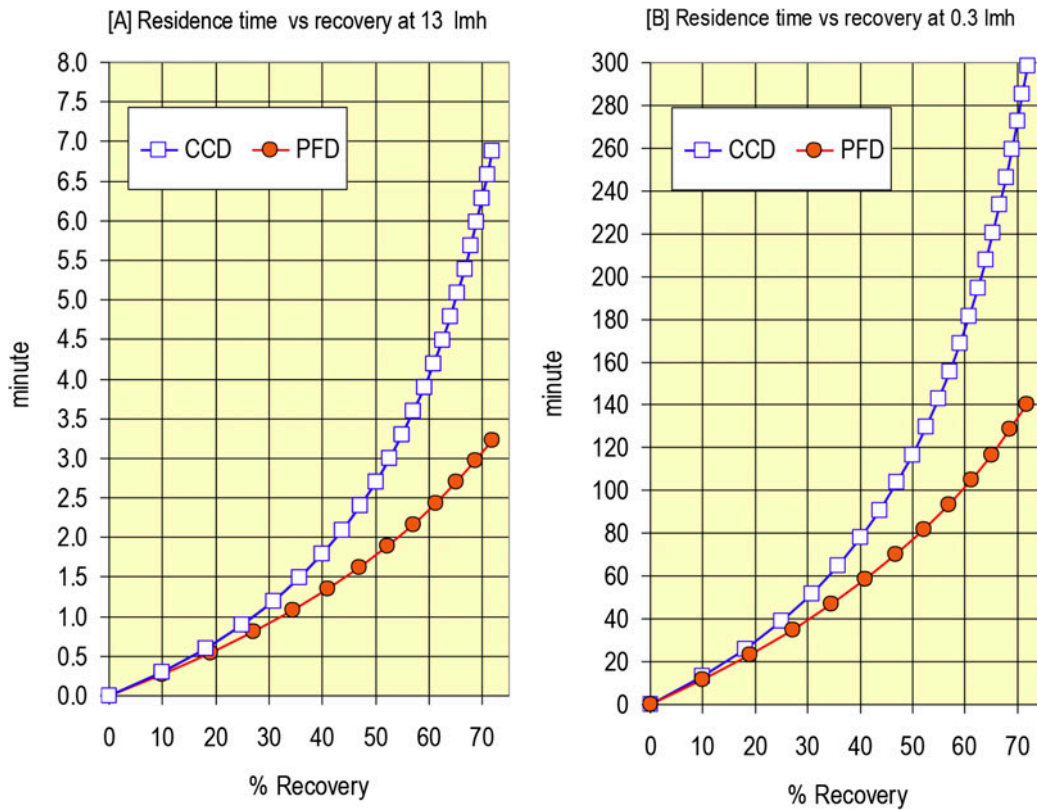


Fig. 8. Residence time vs. recovery for 13 lmh (A) and 0.3 lmh (B) according to the simulation database in Table 1(AB).

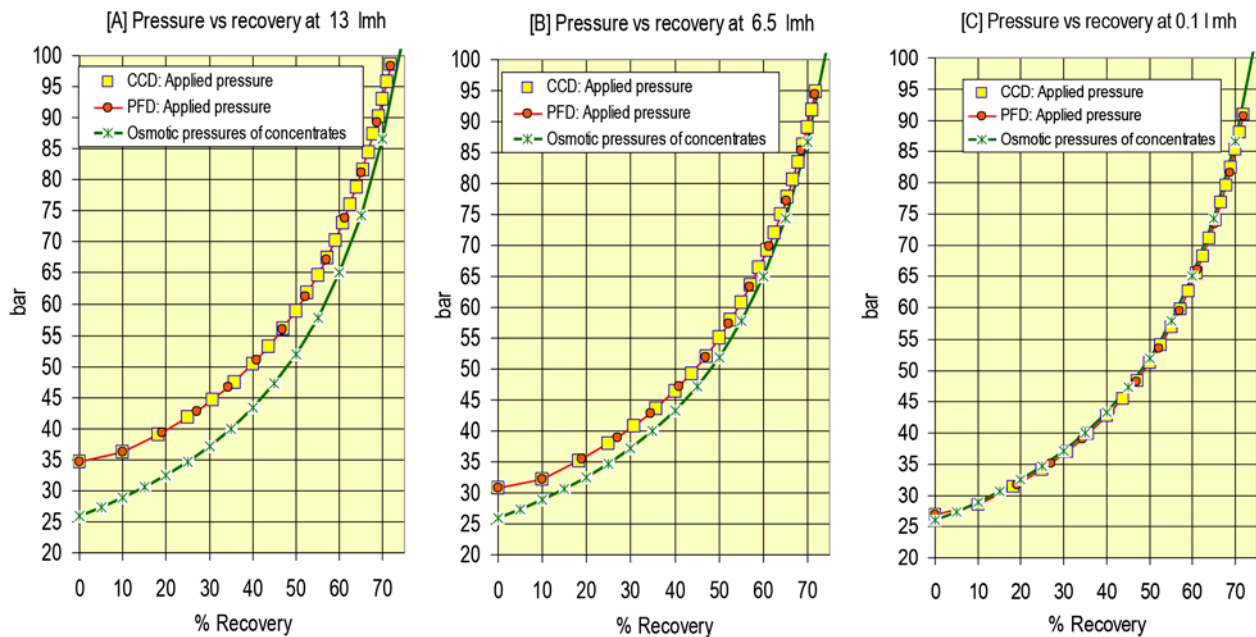


Fig. 9. Pressures vs. recovery for flux of 13 lmh (A), 6.5 lmh (B), and 0.1 lmh (C) with absolute efficiency (100%) of pumps according to the modified simulation database in Table 1(AB).

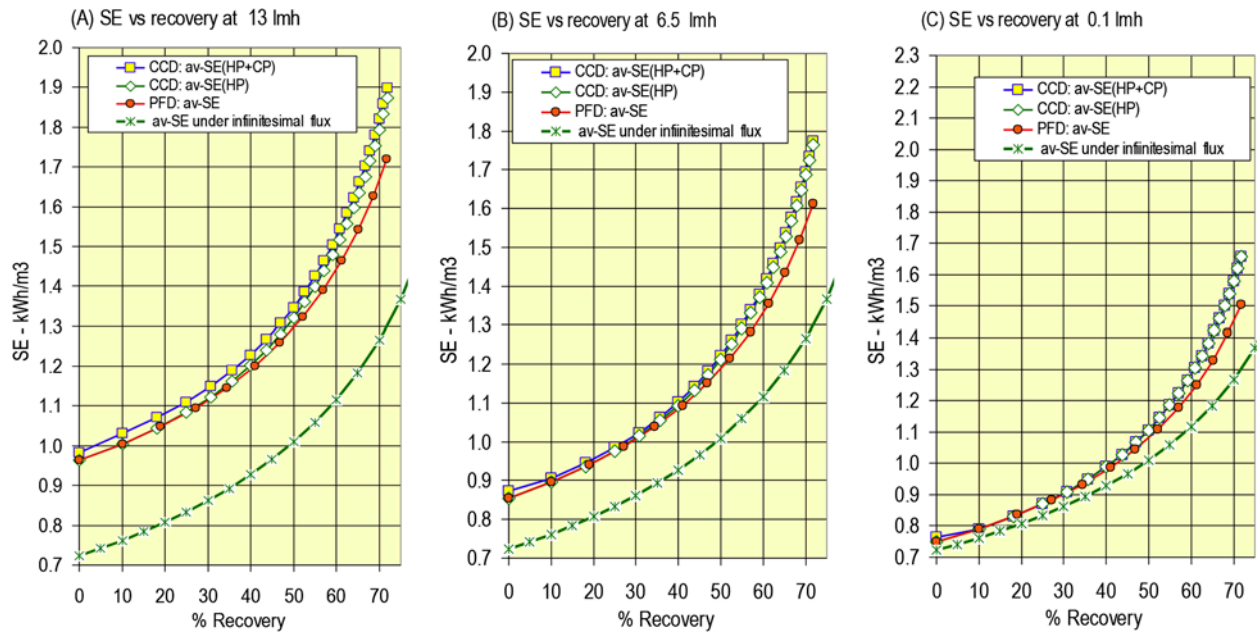


Fig. 10. Specific energies vs. recovery for flux of 13 lmh (A); 6.5 lmh (B), and 0.1 lmh (C) with absolute efficiency (100%) of pumps according to the modified simulation database in Table 1(AB).

Table 2
Typical data of energy and EE for seawater RO desalination

Method	Module	SW (%)	REC (%)	HP eff. (%)	Flux lmh	W_{LM} SE $_{LM}^a$ (kWh/m ³)	W_{SEP} SE $_{SEP}^b$ (kWh/m ³)	Entropy Effi. ^c (%)	SE $_{SEP}^b$ Refs.
SWRO-PFD Theory	ME8	3.5	40	85	13	0.725	2.35	33.6	[2]
SWRO-PFD Perth Australia	ME8	3.5	50	85	13	0.724	2.46	32.1	[28]
SWRO-PFD Palmachim	ME8	4.0	50	85	13	0.828	2.75	32.8	[29]
SWRO-PFD Askelon Israel	ME8	4.0	50	85	13	0.828	2.8	32.2	[4]
SWRO-PFD Hedera Israel	ME8	4.0	50	85	13	0.828	2.9	31.1	[4]
SWRO-CCD [SWC6] Israel	ME4	4.0	50	85	13	0.828	2.12	42.6	[5,6]
SWRO-CCD [SWC6] Israel	ME4	3.5	50	85	13	0.724	1.82	43.4	[5,6]
SWRO-CCD [NanoH20] Israel	ME4	3.5	50	85	13	0.724	1.72	45.9	[14]

^aLeast minimum LM separation work (W) or energy (SE)

^bSeparation (SEP) work (W) or energy (SE)

^cEntropy Efficiency = $100 \times W_{LM}/W_{SEP}$

single-element module and the perfect multi-stage PFD design (Fig. 1(B)) of many such single-element modules with minor energy difference (Fig. 4(A) and (B)) between them in favor of the latter due to the energy requirements of the CP pump in CCD. This study also distinguishes between number of steps required to reach a specified recovery (Fig. 7(A) and (B)) showing that more CCD cycles than PDF stages in a multi-stage design are necessary to reach the same

recovery and this is due to the mixing effect of recycled concentrates with fresh feed at module inlet in the former process. Another feature revealed by the comparative study is that permeates (Fig. 6(A) and (B)) of CCD are of greater TDS compared with those of the multi-stage PFD process. Correlation of results for the exemplified CCD and multi-stage (parentheses) processes for seawater desalination of 50% recovery at 13 lmh flux according to the data in Table 1(AB) and

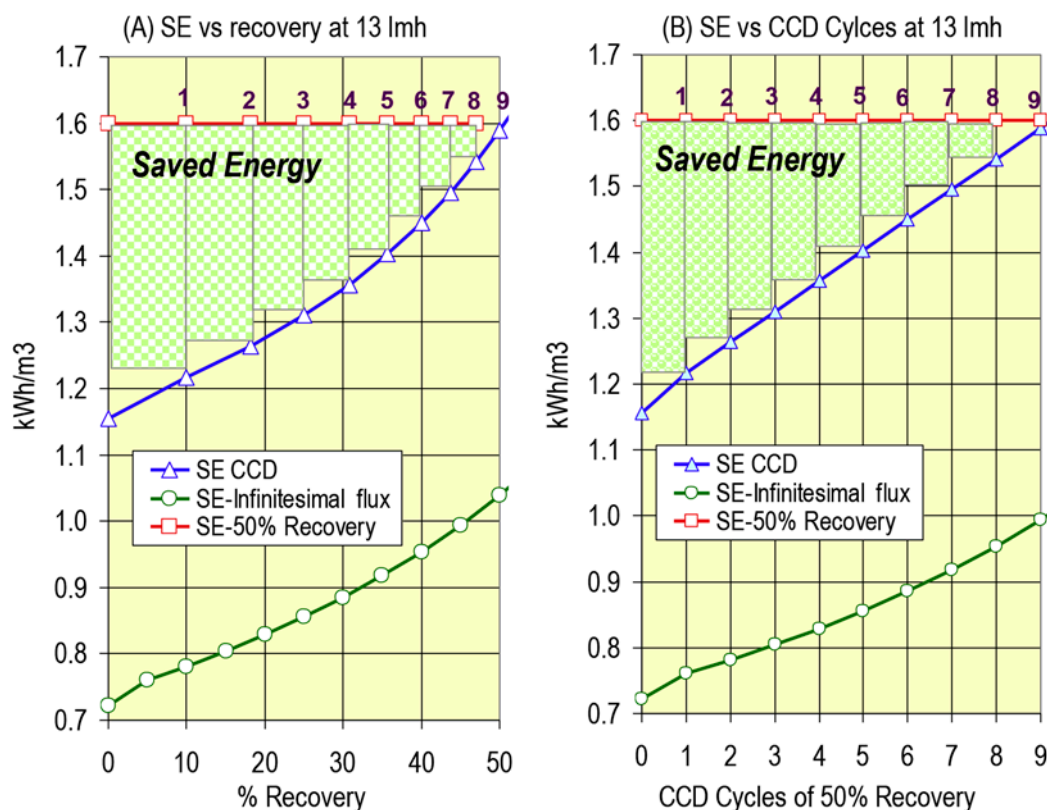


Fig. 11. Origin of saved energy in CCD as a function of recovery (A) and CCD cycles (B) for seawater (3.5%) desalination with 13 lmh flux, 10% MR, 85% eff_{HP} , and 75% eff_{CP} according to the simulation database in Table 1A.

the relevant figures (Figs. 3(A)–8(A)) reveal the followings: 58.9 (58.9) bar applied pressure; 1.59 (1.53) kWh/m³ specific energy; 45.5 (47.5)% EE; 330 (280) ppm average TDS of permeates; 10 (6.5) number steps CCD cycles and PFD stages; and 2.7 (1.8) minute residence time in system.

The simulation database in Table 1(AB) is of general application and may apply to compare CCD and multi-stage PFD processes of identical modules containing more than one element by adjusting the appropriate database parameters such as related to the type of membrane element, number of elements per module, length of pressure vessel, source salinity and its osmotic pressure, flux of operation, module recovery, efficiency of pumps, and temperature. For example, a comparative analysis for 50% seawater desalination recovery at 13 lmh through CCD and the multi-stage PFD processes with the adjusted simulation database in Table 1(AB) for identical four-element modules (ME4) and 25% module recovery reveals the following results with PFD data in parenthesis: 54.7 (56.4) bar applied pressure; 1.622 (1.609) kWh/m³ specific energy; 44.5 (45.08)% EE; 322 (298) ppm average TDS of permeates; 3 (2.5) number of steps; 2.2 (1.4) minute

residence time in system. The results of the exemplified model analysis with ME4 modules regarding the specific energy of CCD confirm that this process proceeds with exceptionally low energy just 0.023 kWh/m³ higher than that of the analogous multi-stage PFD process. Moreover, the comparative simulated CCD and multi-stage PFD (in parentheses) energies of 1.59 (1.53) kWh/m³ for ME and 1.622 (1.609) kWh/m³ for ME4 reveal a slight advantage for the multi-stage PFD over CCD, as well as a small increase in energy by moving from ME to ME4 configurations. The small energy differences of the compared processes clearly confirm that CCD behaves as a nearly perfect multi-stage irrespective of the number of elements per module.

The same simulations applied in this comparative study for the ME and ME4 modules are of general application also for other modules of different number of element and the validation of such theoretical projections requires experimental data for confirmation. The comparative model simulations of the ME and ME4 modules for seawater desalination of 50% recovery at 13 lmh show very small energy differences between them, and since the multi-stage PFD

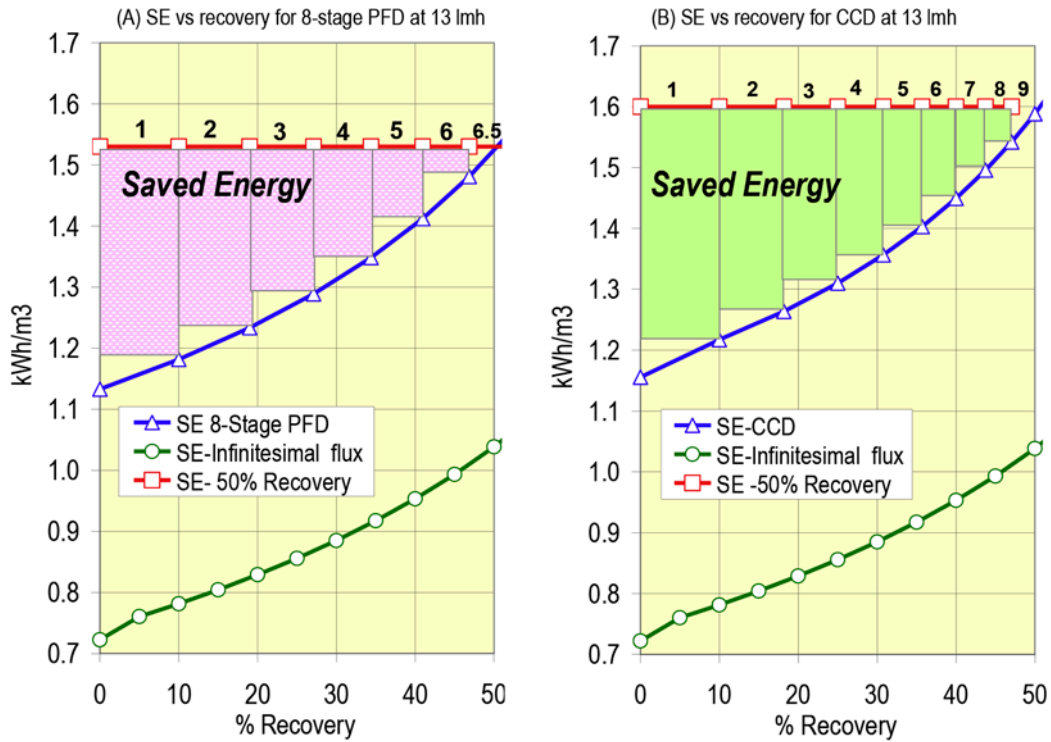


Fig. 12. Energy saved by CCD compared with that of multi-stage PFD as a function of recovery and step-number for seawater (3.5%) desalination with 13 lmh flux, 10% MR, 85% eff_{HP} , and 75% eff_{CP} according to the simulation database in Table 1(AB).

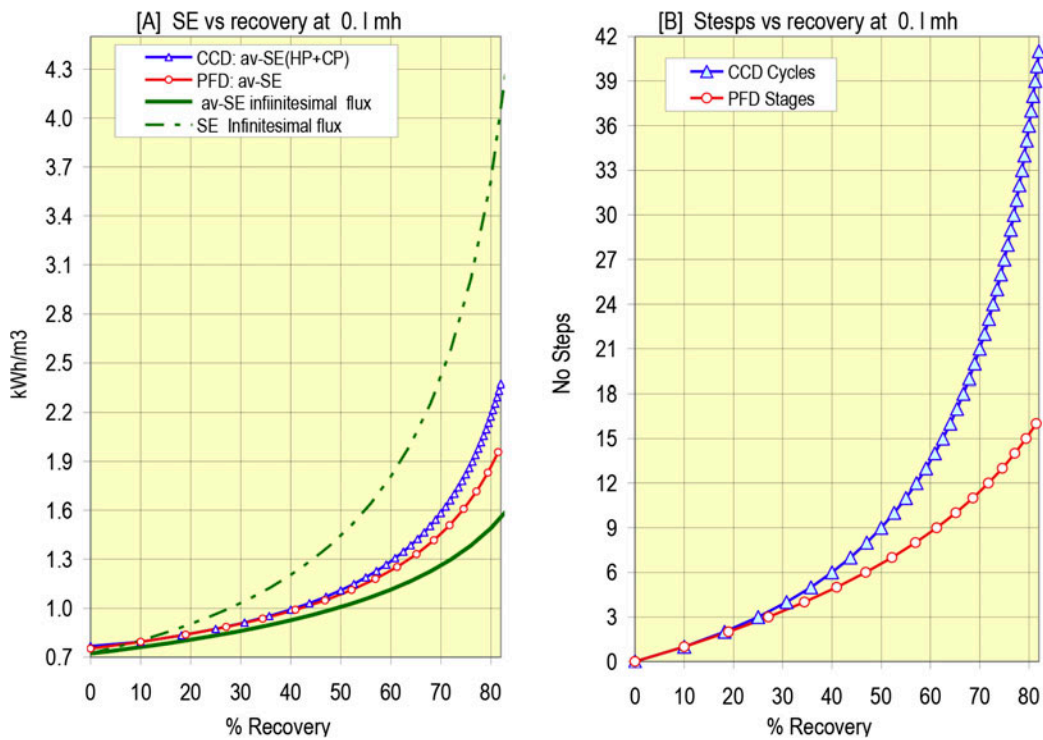


Fig. 13. Energy (A) and step number (B) dependence on recovery for the CCD and multi-stage PFD processes under near-infinitesimal flux (0.1 lmh).

processes proceed with near-absolute energy conversion efficiency, the same should also be true for CCD provided that such a conclusion could be validated experimentally. In this context, noteworthy are the reported [5,6] energy results (e.g. 2.12 kWh/m³) of the 4ME4 ($E = \text{SWC6}$) unit for 50% desalination of Mediterranean water (4.0%) at 15 l/mh flux which translates to 1.69 kWh/m³ when extrapolated to ocean seawater (3.5%). A more recent study reported [14] the application the same 4ME4 unit with Qfrx-SW-365-ES elements [26], instead of SWC6 [27], for the desalination of seawater in the salinity range 33,801–37,197 ppm; flux range 9.2–13.5 l/mh; and recovery range 42–53%, and the results of these trials revealed the specific energy range of 1.453–1.775 kWh/m³. A specific trial in this series with 35,329 ppm seawater at 9.22 l/mh flux and recovery of 47% revealed energy of 1.453 kWh/m³ associated with 50% EE which at present time is a record low. Another specific trial in this series with 33,913 ppm seawater at 12.2 l/mh flux and recovery of 53% revealed [14] the energy of 1.775 kWh/m³ with 39.4% EE as expected by increased flux and recovery. The experimental energy results of said study are the lowest energies reported thus far for ocean seawater and correspond to 45.3–51.7% EE in the recovery range 42–47%. The aforementioned CCD experimental results clearly validate the model simulation database in Table 1A and its trustworthy energy projections as well as that CCD is the method of lowest practical energy pathway to seawater desalination, just slightly above the ideal projections of the multi-stage PFD configuration which is economically prohibited. The typical data of energy and EE for seawater RO desalination in Table 2 demonstrate the exceptional performance of near-absolute energy conversion efficiency of CCD even with modules of four elements compared with the widely used conventional techniques with modules of eight elements.

The origin of saved energy in CCD for seawater (3.5%) desalination with 13 l/mh flux, 10% MR, 85% eff_{HP} , and 75% eff_{CP} is displayed in Fig. 11(A) and (B) as function of recovery (A) and number of CCD cycles (B). Nine CCD cycles (Fig. 11(B)) are required to reach 50% recovery and the declined energy saving is a linear function of the number of CCD cycles. Energy saving on the recovery scale still requires the same nine cycles (Fig. 11(A)) with declined saving being exponential rather than linear. The aforementioned illustrates the meaning of CCD exponential energy consumption as function of recovery (Fig. 11A) versus linear energy consumption as function of cycles (Fig. 11B).

The compared origin of saved energy between CCD and the eight-stage PFD processes, both with the

same single-element modules, for seawater (3.5%) desalination with 13 l/mh flux, 10% MR, 85% eff_{HP} , and 75% eff_{CP} is displayed in Fig. 12(A) and (B) as a function of recovery. CCD proceeds by nine cycles of declined energy saving weight (Fig. 12(B)) from a maximum of ~1.60 kWh/m³, whereas the multi-stage PFD process proceeds by ~6.5 identical stages of saved energy (Fig. 12(A)) from a maximum of ~1.53 kWh/m³. The slightly higher CCD maximum energy (1.60 instead 1.53 kWh/m³) manifests a small energy contribution by the CP in the design (Fig. 1(C)). The increased number of CCD cycles compared with PFD stages (9 compared with 6.5) required to reach 50% in the light of the small maximum energy difference between them in favor of the latter, creates a net effect of near-identical energy savings by both. According to the comparison in Fig. 12(A) and (B), recovery in the CCD and multi-stage PFD processes proceeds by different steps of concentrate recycling with feed blending in the former and by stages without feed blending in the latter, and reaching a defined recovery requires a greater number of cycles than stages.

The greater complexity of CCD compared with multi-stage PFD is also associated with the batch characteristic of the former of increased frequency of cycles and residence time with recovery which translate to greater average specific energy compared with the former. For instance, reaching 50% recovery by CCD at 13 l/mh requires nine cycles (Fig. 7(A)) with residence time of 2.7 min (Fig. 8(A)) compared with 6.5 stages of 1.8 min residence time experienced by the multi-stage PFD process under the same flux and recovery conditions. These differences are manifested in CCD, the higher specific energy [1.60 instead 1.53 kWh/m³—Fig. 12(A) and (B)], lower EE [45.0 instead 47.5%—Fig. 5(A)], and higher average TDS of permeates [330 instead 280 ppm—Fig. 6(A)] compared with multi-stage PFD under the same flux and recovery conditions. The aforementioned considerations also imply increased spread of cited parameters between CCD and multi-stage PFD with increased recovery under the same flux conditions.

The dependence of energy and step-number on recovery for the CCD and multi-stage PFD processes of same single-element module design under near-infinitesimal flux (0.1 l/mh) and absolute efficiency (100%) of pumps derived from the simulation database in Table 1(AB) is displayed in Fig. 13(A) and (B). The av-SE terms for CCD and the multi-stage processes in Fig. 13(A) express the average along the recovery (R) progression and takes into account the number of steps (N) required to reach a specific recovery (Fig. 13(B)), with SE at infinitesimal flux expressed by $26/36/(1-R/100)$, and the av-SE by $26/36/(1-R/$

100)/ N kWh/m³. N for CCD stands for closed-circuit cycles and for stages in the multi-stage PFD process. The SE infinitesimal flux expression describes the minimum energy requirements of a single-stage single-pass process with a perfect module comprising multiple elements. The data in Fig. 13(A) and (B) clearly reveal the dependence of average minimum CCD and PFD energy on N steps (cycles or stages) with increased frequency of N on the recovery scale resulting with higher energy, and such an increase in N is also associated with an increased residence time in the system. The trend shown in Fig. 13(A) is of increased minimum energy of CCD compared with that of multi-stage PFD as a function of recovery with negligible differences up to 40%, ~0.02 kWh/m³ at 50%, ~0.06 kWh/m³ at 60%; ~0.13 kWh/m³ at 70%, and ~0.30 kWh/m³ at 80% and it can be clearly seen in Fig. 13(B) that the increase difference is associated with a greater frequency of CCD cycles compared with lower frequency of PFD stages.

A recently reported study by Lin and Elimelech [25] analyzes the CCD and multi-stage PFD processes for SW and BW. The projected SW energy results of infinite stages (∞) of this study show the same trend found in Fig. 13(A), but with a greater separation between the multi-stage PFD and CCD as a function of recovery above 40% such as ~0.12 (0.02) kWh/m³ at 50%, ~0.19 (0.06) kWh/m³ at 60%; ~0.38 (0.13) kWh/m³ at 70%, and ~0.87 (0.30) kWh/m³ at 80%—data in parentheses pertain the present study. It should be pointed out that in the current model study, the number of CCD cycles above 40% recovery meets the step number $N > 8$ of near or infinite (∞) conditions. A plausible explanation of the projected difference energy spread may arise from the application of an insufficiently rigorous CCD model in the reported study [25] to enable clear distinction between CCD cycles and PFD stages as is done in the current study. The current study makes use of a rigorous CCD simulation database of general applications for SW and BW desalination performance projections of different module designs MEn ($n = 1-4$) with results found within $\pm 2\%$ of experimental data.

6. Concluding remarks and outlook

Rigorous theoretical model simulations of the CCD and multi-stage PFD designs for seawater with the same single-element modules (ME) in the flux range 13.0–0.1 lmh reveal that the former under fixed flow and variable pressure conditions behaves as a near-perfect multi-stage PFD design and allows to desalinate seawater with exceptionally low-energy and high-energy conversion efficiency without the need for

energy recovery compared with conventional single-pass PFD techniques with modules of eight elements. The energy consumption is exemplified in the commonly practiced flux (13 lmh) as well as under near-infinitesimal flux (0.1 lmh) of minimum SE conditions. While multi-stage SWRO-PFD desalination is economically prohibited due to high construction costs, simple low-cost CCD units such as 4MEn ($n = 1-4$) were already demonstrated for Mediterranean (4.0%) and ocean (3.5%) waters with record low energy consumption at 50% recovery of 2.12 and 1.72 kWh/m³, respectively, of near-absolute energy conversion efficiency and improved EE of ~35% compared with conventional techniques without the need for ERD. In the light of the increased reliance on SW desalination for production of freshwater supplements on large scale in various worldwide regions, and since energy cost is the principle component in the price of seawater permeate, the reduction in SWRO desalination energy is a major future goal of the desalination industry and the recently emerging CCD technology makes such a goal attainable already today.

Acknowledgments

Funds to Desalitech Ltd. by AQUAGRO FUND L.P. (Israel) and by Liberation Capital LLC (USA) and Spring Creek Investments (USA) are gratefully acknowledged.

References

- [1] M. Elimelech, W.A. Phillip, The future of seawater desalination: Energy, technology, and the environment, *Science* 333 (2011) 712–717.
- [2] K.H. Mistry, R.K. McGovern, G.P. Thiel, E.K. Summers, S.M. Zubair, J.H. Lienhard V, Entropy generation analysis of desalination technologies, *Entropy* 13 (2011) 1829–1864.
- [3] S. Loeb, S. Sourirajan, Sea water demineralization by means of an osmotic membrane, *Am. Chem. Soc. Adv. Chem. Ser. ACS* 38 (1963) 117–132.
- [4] N. Voutchkov, Membrane Seawater Desalination—Overview and Recent Trends, IDA Conference, Riverside, CA, USA, 2–3 November 2010.
- [5] A. Efraty, R.N. Barak, Z.I. Gal, Closed circuit desalination—A new low energy high recovery technology without energy recovery, *Desalin. Water Treat.* 31 (2011) 95–101.
- [6] A. Efraty, R.N. Barak, Z. Gal, Closed circuit desalination series no-2: New affordable technology for sea water desalination of low energy and high flux using short modules without need of energy recovery, *Desalin. Water Treat.* 42 (2012) 189–196.
- [7] A. Efraty, Closed circuit desalination series no-6: Conventional RO compared with the conceptually different new closed circuit desalination technology, *Desalin. Water Treat.* 41 (2012) 279–295.

- [8] A. Efraty, Closed circuit desalination series no. 8: Record saving of RO energy by SWRO-CCD without need of energy recovery, *Desalin. Water Treat.* 52(31–33) (2014) 5717–5730.
- [9] A. Efraty, CCD Series No-11: Single module compact SWRO-CCD units of low energy and high recovery for seawater desalination including with solar panels and wind turbines, *Desalin. Water Treat.* 53(5) (2015) 1162–1176.
- [10] A. Efraty, CCD Series No-13: Illustrating low energy SWRO-CCD of 60% recovery and BWRO-CCD of 92% recovery with a single element module without ER means—A theoretical extreme case study *Desalin. Water Treat.* doi: [10.1080/19443994.2015.1035495](https://doi.org/10.1080/19443994.2015.1035495).
- [11] A. Efraty, CCD Series No-14: SWRO-CCD under fixed-pressure and variable flow compared with fixed-flow and variable pressure conditions, *Desalin. Water Treat.* 56(4) (2015) 875–893.
- [12] A. Efraty, CCD Series No-15: Simple design batch SWRO-CCD units for high recovery and low energy without ERD over a wide flux range of high cost effectiveness, *Desalin. Water Treat.* doi: [10.1080/19443994.2015.1035496](https://doi.org/10.1080/19443994.2015.1035496).
- [13] A. Efraty, CCD Series No-16: CCD Series No-16: Opened versus closed circuit SWRO batch desalination for volume reduction of silica containing effluents under super-saturation conditions, *Desalin. Water Treat.* doi: [10.1080/19443994.2015.1035494](https://doi.org/10.1080/19443994.2015.1035494).
- [14] Z. Gal, A. Efraty, CCD Series No-18: Record low energy in closed circuit desalination of ocean seawater with NanoH₂O elements without ERD, *Desalin. Water Treat.* doi: [10.1080/19443994.2015.1035500](https://doi.org/10.1080/19443994.2015.1035500).
- [15] A. Efraty, Closed circuit desalination series no-3: High recovery low energy desalination of brackish water by a new two-mode consecutive sequential method, *Desalin. Water Treat.* 42 (2012) 256–261.
- [16] A. Efraty, Closed circuit desalination series no-4: High recovery low energy desalination of brackish water by a new single stage method without any loss of brine energy, *Desalin. Water Treat.* 42 (2012) 262–268.
- [17] A. Efraty, J. Septon, Closed circuit desalination series no-5: High recovery, reduced fouling and low energy nitrate decontamination by a cost-effective BWRO-CCD method, *Desalin. Water Treat.* 49 (2012) 384–389.
- [18] A. Efraty, Z. Gal, Closed circuit desalination series No 7: Retrofit design for improved performance of conventional BWRO system, *Desalin. Water Treat.* 41 (2012) 301–307.
- [19] A. Efraty, Closed circuit desalination series No-9: Theoretical model assessment of the flexible BWRO-CCD technology for high recovery, low energy and reduced fouling applications, *Desalin. Water Treat.* 53(7) (2015) 1755–1779.
- [20] A. Efraty, CCD Series No-10: Small compact BWRO-CCD units of high recovery, low energy and reduced fouling for supplied water upgrade to industry, irrigation, domestic and medical applications, *Desalin. Water Treat.* 53(5) (2015) 1145–1161.
- [21] A. Efraty, Closed circuit desalination series no-12: The use of 4, 5 and 6 element modules with the BWRO-CCD technology for high recovery, low energy and reduced fouling applications, *Desalin. Water Treat.* 53 (7) (2015) 1780–1804.
- [22] J. Septon, A. Efraty, CCD Series No-17: Application of the BWRO-CCD technology for high recovery low energy desalination of domestic effluents, *Desalin. Water Treat.*, doi: [10.1080/19443994.2015.1035498](https://doi.org/10.1080/19443994.2015.1035498).
- [23] Z. Gal, J. Septon, A. Efraty, A.-M. Lee, CCD Series no-20: High flux low energy upgrade of municipal water supplies with 96% recovery for boiler-feed and related applications *Desalin. Water Treat.* doi: [10.1080/19443994.2015.1126413](https://doi.org/10.1080/19443994.2015.1126413).
- [24] V. Sonera, J. Septon, A. Efraty, CCD series no-21: Illustration of high recovery (93.8%) of a Silica containing (57 ppm) source by a powerful technology of volume reduction prospects, *Desal. Water Treat.* doi: [10.1080/2015.1126412](https://doi.org/10.1080/2015.1126412).
- [25] S. Lin, M. Elimelech, Staged reverse osmosis operation: Configuration, energy efficiency, and application potential, *Desalination* 366 (2015) 4–9.
- [26] Available from: <http://www.nanoh2o.com/files/qfx%sw%20400%20es%204-9-12.pfd>.
- [27] Available from: <http://www.membranes.com/docs/8inch/SWC6.pdf>.
- [28] M.A. Sanz, R.L. Stover, Low energy consumption in the Perth Seawater Desalination Plant, MP07, IDA World Congress, Maspalomas, Gran Canaria—Spain, 21–26 October 2007.
- [29] A. Hermoni, Actual energy consumption and water cost for the SWRO systems at Palmachim—Case history, IDA Conference, Riverside, CA, USA, 2–3 November 2010.